Effects of Bentonite on the Dielectric Properties of High- Pressure Polyethylene

Matanat Mehrabova[1,2], Kamal Gulmammadov[1] and Rafig Sadigov[1,3]

[1]Azerbaijan Technical University, 25 H.Javid Avenue, Baku, AZ1073, Azerbaijan
[2]Institute of Physics, Ministry of Science and Education, 131, H.Javid ave., AZ-1073, Baku, Azerbaijan
[3]Azerbaijan State University of Economics, Baku, Azerbaijan
metanet.mehrabova@aztu.edu.az

Abstract. Composites based on high-pressure polyethylene reinforced with a bentonite filler were developed and analyzed. The defined significant frequency-dependent dispersion of the dielectric parameters is attributed to the migration of intrinsic point defects, such as vacancies, interstitial atoms, and structural defects within the filler sublattice. These findings highlight the critical role of both filler content and defect dynamics in determining the electrical performance of HPPE-based composites. The temperature dependence of the permittivity ε of the composites indicates that permittivity exhibits a steady increase with rising temperature, indicating enhanced polarization mechanisms at elevated temperatures. Dielectric loss tangent behavior is characterized by a more complex, non-monotonic trend. The observed distinct maxima suggested the presence of thermally activated processes, and peaks are likely associated with changes in the structural parameters of the interphase boundary layer, which may arise due to phase transitions occurring within the filler crystals.

Keywords: high-pressure polyethylene, bentonite, dielectric properties, frequency dispersion, defects.

1 Introduction

The advancement of the technique necessitated the enhancement of material properties and the adoption of novel materials [1-5]. One of the promising areas of recent years in polymer science is the development of principles for obtaining and studying polymer composites and nanocomposites[6-8]. An important advantage of composites is their higher functionality and electrical stability compared to polymer analogues. The functioning of composite structures as an active element is associated, in particular, with charge formation phenomena. Therefore, when developing new dielectric composites, researchers' attention is mainly focused on obtaining and studying dielectric properties under various influences (temperature, frequency and etc.) [9-16]. These studies can serve as a basis for selecting components of compositions for obtaining elements with predetermined parameters and assessing the possibility of their use in dielectric systems.

Analysis of literature data shows that fillers impart increased thermal and electrical conductivity, new magnetic properties to polymeric materials, improve mechanical and

R. Rzayev et al. (eds.), *Proceedings of the International Conference on Current Problems in Engineering and Applied Sciences (ICCPEAS 2025)*, Advances in Engineering Research 299,
https://doi.org/10.2991/978-94-6239-668-5_30

electrical strength, and influence a number of other functional parameters. The use of bentonite is of particular interest in the development of new types of composite materials. The choice of bentonite as a filler is due not only to its natural abundance and cost-effectiveness, but also to the limited exploration of its electrophysical characteristics, along with its potential for forming sufficiently elastic thin-film composites. Composites with natural bentonite fillers can exhibit a wide range of useful properties and be successfully applied in various industrial sectors [17-19].

Bentonite (B), a layered aluminosilicate with high cation exchange capacity and surface activity, can interact effectively with polymer matrices, especially when properly exfoliated or intercalated. When introduced in small amounts (typically 2–8 wt%), bentonite can enhance the dielectric strength, reduce permittivity losses, and increase mechanical robustness of the resulting composite. These effects are attributed to its ability to act as a barrier to charge carrier movement and to its reinforcement of the polymer structure at the nanoscale [20].

Mechanical testing of bentonite-filled composites confirms the potential of this material to increase modulus and tensile strength while maintaining adequate flexibility. This is particularly relevant for film-type materials, where mechanical integrity under thermal and electrical stress is critical. Furthermore, bentonite contributes to improved thermal stability due to its layered structure, which hinders the mobility of polymer chains and retards thermal degradation processes.

The dielectric response of bentonite-containing composites is known to be frequency- and temperature-dependent, typically exhibiting improved stability across a broad operational range. This behavior makes such composites suitable candidates for insulating layers in electronic devices, flexible electronics, and electrothermal applications.

Overall, the study of dielectric and mechanical properties of polymer composites with bentonite fillers opens up new directions in materials engineering. By optimizing the filler concentration, particle dispersion, and surface modification techniques, it is possible to design composite materials with tailored properties for specific electrical and mechanical applications.

Bentonite, a naturally occurring clay mineral composed predominantly of montmorillonite, has gained increasing attention as functional filler in polymer composites due to its layered structure, high surface area, and ion-exchange capacity. In recent years, bentonite has been explored as an effective additive for enhancing both the dielectric and mechanical properties of polymer-based composites, particularly for applications in insulation, packaging, and structural materials.

The incorporation of bentonite into polymer matrices has been shown to influence dielectric behavior significantly. The dielectric constant (ε') of bentonite-filled composites generally increases with filler content due to the polar nature of the bentonite particles and their ability to store electric charge at the interfaces. However, excessive filler loading can lead to agglomeration and interfacial defects, resulting in dielectric loss and reduced breakdown strength. Optimal dispersion and interfacial bonding between the polymer matrix and bentonite particles are therefore critical to maintaining favorable dielectric performance.

Mechanical testing of bentonite-reinforced composites also demonstrates substantial improvements in tensile strength, modulus, and impact resistance at low filler concentrations. These improvements are attributed to the effective stress transfer

between the polymer and the rigid bentonite particles, along with enhanced interfacial adhesion. At optimal filler loadings—typically in the range of 3–10 wt% a balance between stiffness and toughness is achieved. Beyond this range, the mechanical benefits may plateau or even decline due to particle aggregation and poor stress distribution.

The degree of enhancement in both dielectric and mechanical properties strongly depends on factors such as bentonite particle size, surface modification (e.g., organophilization), and processing techniques. Surface modification, in particular, improves compatibility with hydrophobic polymer matrices, promoting better dispersion and improved interfacial interactions.

Thus, bentonite serves as a multifunctional filler that can enhance both the dielectric and mechanical performance of polymer composites when used in appropriate concentrations and under optimized processing conditions. These composites hold promise for applications in electrical insulation, flexible electronics, structural components, and environmentally sustainable materials.

Numerous studies [21,22] have demonstrated that incorporating bentonite fillers into high-pressure polyethylene (HPPE) significantly influences the dielectric properties of the resulting composites. In particular, both the relative permittivity (ε_r) and the dielectric loss tangent ($\tan\delta$) typically increase with higher bentonite content. This behavior is primarily attributed to enhanced interfacial polarization and increased charge carrier mobility at the filler–polymer interface.

Authors [23-26] indicate that LDPE + bentonite composites show improved dielectric performance at low filler concentrations (3–7 wt%), with increased permittivity and controlled dielectric loss. However, excess filler leads to aggregation, increased loss, and reduced electrical insulation quality. The interfacial polarization and filler dispersion play major roles in determining the final dielectric behavior.

The aim of the present study is to synthesize and investigate the frequency temperature dependence of dielectric properties of composites based on high pressure polyethylene (HPPE) with additives bentonite $(HPPE)_{1-x}(Bentonite)_x$ in a large range filler concentrations 5-80wt%.

2 Materials and methods of experiment

Composites were fabricated using high pressure polyethylene grade 10803-020 and bentonite as the primary components. Both the bentonite and HPPE were used in powder form. The powders were pre-ground in a ball mill with porcelain grinding media until the particle size was reduced to ≤60 μm. The composite mixtures were then homogenized and subjected to hot pressing at a temperature of 140 -150°C under a pressure of 15 MPa. The composition of the composites varied across a broad range, with HPPE content from 95 to 20 wt.% and bentonite content from 5 to 80 wt.% . The resulting samples had an average thickness of approximately 150 μm. The film thickness uniformity was measured using an optical thickness gauge (model N3B-2) and a micrometer [22].

The surface microrelief of the HPPE+Bentonite composites was analyzed using an Atomic Force Microscope (AFM) of the Solver Next (NT-MDT) model operating in MD mode (Fig. 1).

Fig. 1 The Nanoeducator microscope, operating based on the atomic force microscopy principle.

Electrical properties, including capacitance (C), resistance (R), and dielectric loss (D), were measured with a digital immittance meter (E7-20) over a frequency range of 25–10^6 Hz at a constant temperature of 300 K. A measuring voltage of 1 V was applied to each sample. The instrument automatically selected the appropriate reactive component for modeling the equivalent circuit of each composite.

The real (ε′) and imaginary (ε″) parts of the complex permittivity, along with the specific resistivity (ρ), were calculated from the measured values of C and D according to the established formulas [27].

$$\varepsilon' = \frac{\varepsilon}{\sqrt{1+D^2}} \qquad \varepsilon'' = \frac{\varepsilon}{\sqrt{(1+D^2)}D} \tag{1}$$

$$C = \frac{\varepsilon\varepsilon_0 S}{d} \tag{2}$$

$$\sigma = 2\pi\nu\varepsilon''\varepsilon_0 D \tag{3}$$

The real (ε′) and imaginary (ε″) parts of the complex dielectric permittivity, as well as the electrical conductivity (σ) and specific resistance (ρ), were calculated based on the measured values of capacitance (C) and dielectric loss (D). The dielectric loss D is defined as the tangent of the loss angle:

$$D=\tan\delta=\varepsilon'' / \varepsilon' \tag{4}$$

where ε′ is the real part of the permittivity (related to energy storage) and ε″ is the imaginary part (associated with energy dissipation). The permittivity values were calculated using the standard relations involving the capacitance of the sample, its geometry, and the vacuum permittivity $\varepsilon_0=8.85\times10^{-12}$ F/m.

3 Experimental results and discussion

AFM was employed to evaluate the surface morphology and nanostructure of HPPE-based composites incorporated with varying contents of bentonite (5%, 7%, 10%, and 20% by weight) and study how the bentonite content influences surface roughness, dispersion quality, and interfacial interactions at the nanoscale. AFM was conducted in tapping mode using a silicon cantilever with a nominal radius of ~10 nm. Samples were

cryo-microtomed to obtain smooth cross-sectional surfaces. Scan areas of 5 μm × 5 μm and 1 μm × 1 μm were recorded for each sample to compare both macro- and nano-scale features.

Fig.2- Fig.5 presents the results of the surface microrelief analysis of the composites in both 2D and 3D imaging modes, along with the corresponding histograms. As shown, varying the volume content of bentonit filler leads to noticeable changes in the surface morphology. These changes are likely associated with altered interactions between the polymer matrix and the filler within the interfacial (boundary) layer.

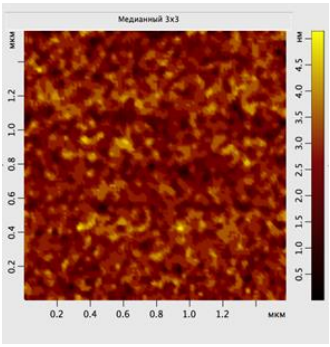

a)

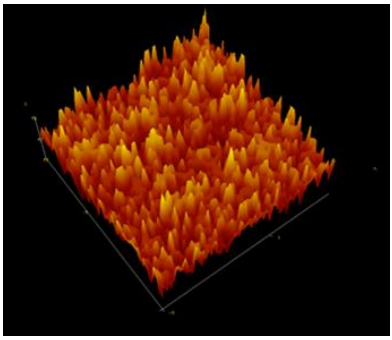

b)

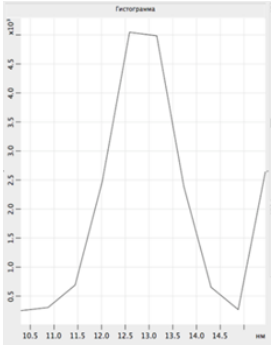

c)

Fig. 2 Microrelief of the surface of $(HPPE)_{1-x}(B)_x$, x = 5% the composite a) 2D images b) 3D images, c) histograms

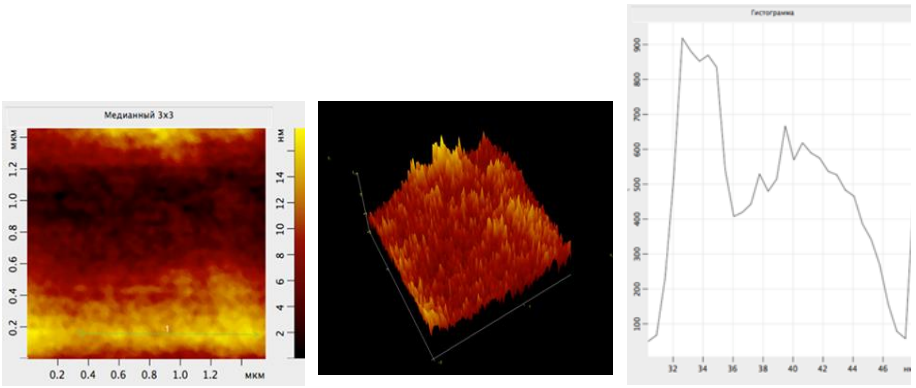

a) b) c)

Fig. 3 Microrelief of the surface of the composite $(HPPE)_{1-x}(B)_x$, x = 7wt%: a) 2D images b) 3D images, c) histograms

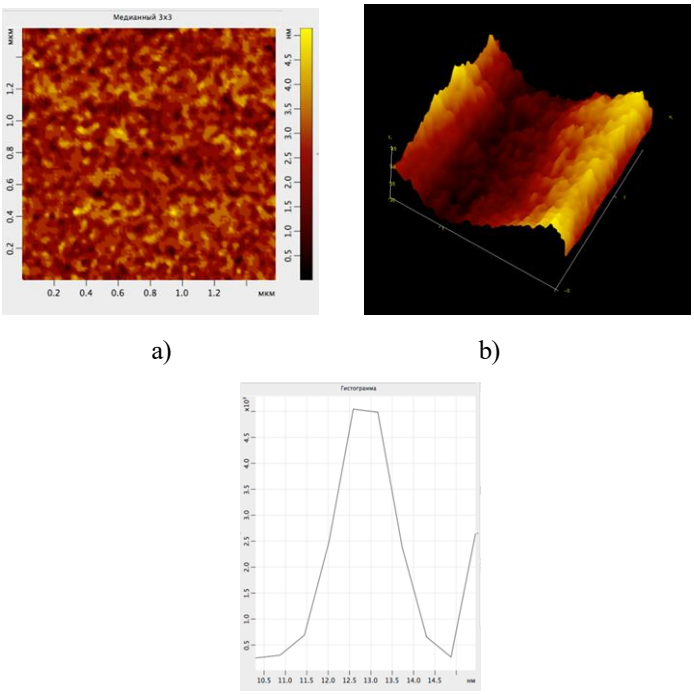

a) b)

c)

Fig. 4. Microrelief of the surface of the composite $(HPPE)_{1-x}$ $(B)_x$, x = 10wt%: a) 2D images b) 3D images, c) histograms

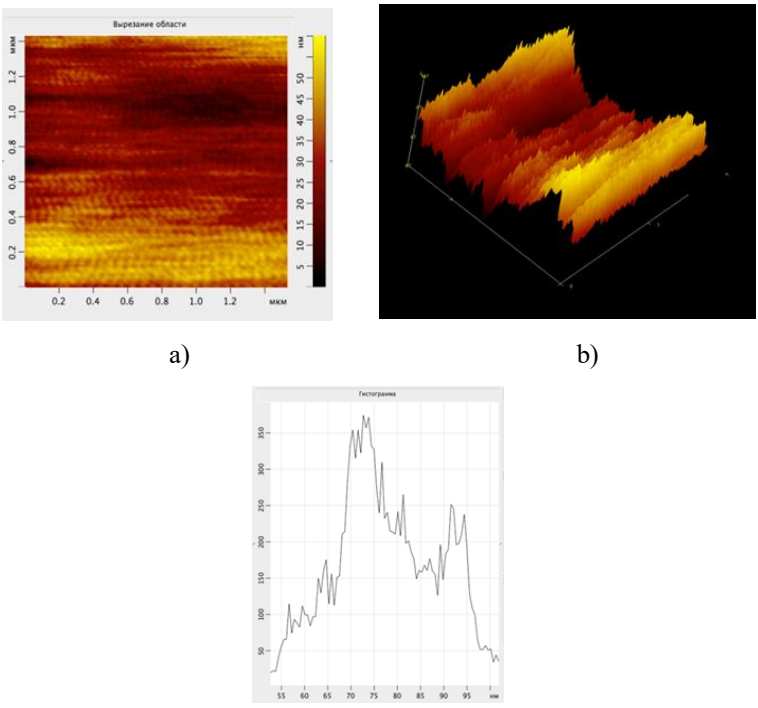

Fig. 5. Microrelief of the surface of the composite $(HPPE)_{1-x}(B)_x$, x = 20%: a) 2D images b) 3D images, c) histograms

Fig. 2 illustrates the AFM analysis of HPPE + 5wt% bentonite composites. The surface topography reveals a relatively smooth surface with minor protrusions, suggesting partial exfoliation of the bentonite within the polymer matrix. The corresponding phase image exhibits moderate contrast, indicating a fair level of dispersion of the bentonite layers. The root mean square (RMS) roughness is approximately 15 nm, confirming the overall surface uniformity. Although a few agglomerated domains are observed, the bentonite appears to be reasonably well-distributed throughout the matrix. The uniform surface morphology implies good interfacial bonding between the HPPE and the bentonite filler at this concentration level.

Fig. 3 presents the AFM analysis of HPPE + 7wt% bentonite composites. Compared to the 5wt% bentonite sample, the surface exhibits increased irregularity, indicating a rougher topography due to the higher filler content. The phase image shows a slight increase in contrast, with the presence of larger domains, suggesting localized agglomeration of bentonite particles. The RMS roughness rises to approximately 20 nm, reflecting this increased surface variation. While the overall dispersion of bentonite remains acceptable, signs of incipient heterogeneity and clustering are evident, potentially affecting the uniformity of the composite structure.

Fig.4 shows the AFM analysis of HPPE + 10wt% bentonite composites. The surface topography reveals a noticeable increase in roughness, accompanied by greater phase contrast compared to lower filler contents. The phase image provides clear

evidence of particle clustering, indicating a decline in dispersion quality. The RMS roughness reaches approximately 30 nm, reflecting the formation of micro-aggregates on the composite surface. At this filler level, the nanofillers begin to form larger agglomerates, which compromises surface homogeneity. These observations suggest that the composite may be approaching a saturation point beyond which effective dispersion becomes increasingly difficult.

Fig. 5 presents the AFM analysis of HPPE + 20wt% bentonite composites. The surface topography is highly irregular, characterized by pronounced peaks and valleys, indicating significant surface distortion. The phase image displays strong contrast, which is indicative of phase separation and poor nanofiller dispersion. The RMS roughness reaches approximately 50 nm, the highest among all samples analyzed. The excessive bentonite content leads to severe agglomeration, likely caused by filler overload and insufficient interfacial adhesion. Such structural inhomogeneity may negatively impact the mechanical performance and integrity of the composite material.

Thus, AFM analysis demonstrates a progressive increase in surface roughness and phase heterogeneity with increasing bentonite content. While 5–7wt% bentonite provides reasonably uniform dispersion, higher loadings (10–20wt%) result in significant aggregation, limiting the effectiveness of filler reinforcement. Optimization around 5–7wt% may offer the best balance between dispersion and property enhancement.

The dielectric properties of high-pressure polyethylene (HPPE) composites with mixed bentonite fillers were investigated in the temperature range of 300–380 K. Composites with filler concentrations up to 80wt% bentonite were studied. As shown in Fig. 6, the dielectric constant of the composites, represented as $(HPPE)_{1-x}(B)_x$, remains relatively unchanged for filler contents up to 50wt%. However, beyond this threshold, a sharp increase in the dielectric constant is observed. At filler concentrations exceeding 50wt% bentonite, the dielectric constant increases by a factor of approximately 20.

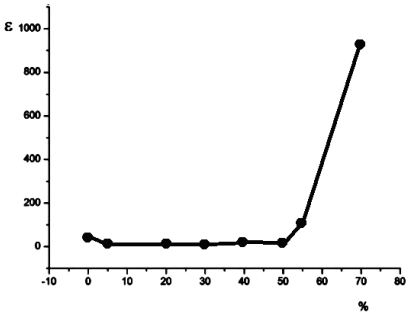

Fig. 6. Dependence of dielectric constant on the percentage content of dispersant.

Fig. 7(a) illustrates the frequency dependence of the permittivity (ε) for the 95wt% HPPE + 5wt% bentonite composite. As observed, the permittivity exhibits a sharp initial decrease up to approximately 200 Hz, followed by a gradual decline from $\varepsilon \approx 5.5$ to 4.8. Interestingly, with a further increase in frequency up to 1000 Hz, ε exhibits a slight rise, increasing from 4.8 to 5.45, indicating a potential relaxation behavior or interfacial polarization effects at higher frequencies.

In contrast, Fig. 7(b) displays the frequency dependence of ε for the 45wt% HPPE + 55wt% bentonite composite. A markedly different behavior is observed: at low

frequencies, even a small increase in frequency causes a sharp drop in permittivity, from approximately 80 to 15. Beyond this sharp decrease, ε remains almost constant across the rest of the frequency range up to 1000 Hz.

It is important to emphasize that increasing the bentonite filler content to 55wt% results in a more than 15-fold increase in the low-frequency permittivity compared to the 5wt% filled composite. This significant enhancement is likely due to interfacial polarization (Maxwell–Wagner–Sillars effect) and the formation of a more continuous filler network, which dramatically alters the dielectric behavior of the composite.

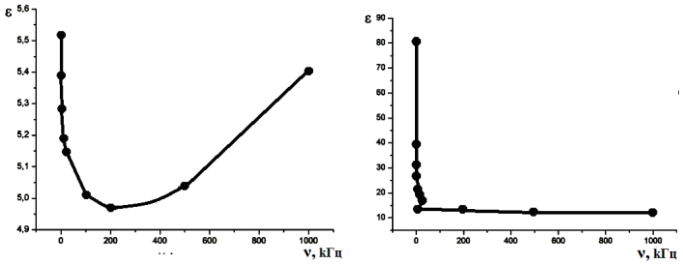

a) b)

Fig.7. Dependence of permittivity on the frequency of an alternating field. a) 95% HPPE+5% B, б) 45% HPPE+ 55% B

Fig. 8 presents the frequency dependence of the imaginary part of the permittivity (ε") for three composite contents: (a) 95wt% HPPE + 5wt% bentonite, (b) 80 wt% HPPE + 20 wt% bentonite, (c) 60 wt% HPPE + 40 wt% bentonite.

As shown in Fig. 8(a), the 95/5 composite exhibits a distinct deep minimum in ε" at low frequencies. Upon increasing the frequency to approximately 200 Hz, ε" increases by an order of magnitude, reflecting enhanced dielectric losses likely due to interfacial polarization. However, as the frequency continues to rise toward 1000 Hz, ε" gradually decreases from 0.5 to 0.18, indicating reduced dipolar relaxation or conductivity effects at higher frequencies.

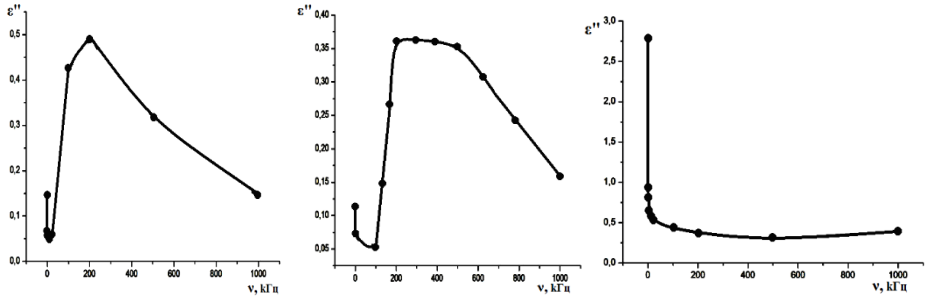

a) б) c)

Fig. 8. Dependence of the imaginary part of the permittivity on the frequency of the alternating field a) 95 wt% HPPE +5wt% B, б) 80 wt% HPPE +20 wt% B, c) 60 wt% HPPE +40 wt% B

Fig. 8(b) illustrates the frequency dependence of the imaginary part of the permittivity (ε") for the 80 wt% HPPE + 20 wt% bentonite composite. The curve exhibits a behavior similar to that of the 95/5 composite shown in Fig. 7(a), but with a shifted minimum occurring at a frequency of 100 Hz. As the frequency increases to 200 Hz, ε" rises sharply from 0.05 to 0.36, reflecting enhanced dielectric losses likely due to charge carrier mobility or interfacial polarization effects. Beyond this point, ε" decreases slightly with increasing frequency and, in the 500–1000 Hz range, drops more notably from 0.35 to 0.16, indicating the onset of relaxation phenomena or a decline in conductive contributions [28.

In contrast, Fig.8(c) shows the behavior of the 60 wt% HPPE + 40 wt% bentonite composite, which differs significantly from the lower-filled systems. At low frequencies, even a small increase in frequency results in a sharp decrease in ε" from 2.8 to 0.5, followed by a plateau where ε" remains nearly constant over a wide frequency range (20–1000 Hz). This response suggests strong interfacial interactions and restricted charge mobility, possibly due to a percolated filler network or saturation of polarizable interfaces.

The observed decrease in both the real and imaginary parts of the permittivity with increasing frequency can be attributed to the inability of various relaxation mechanisms to respond within the time scale of the alternating field. At low frequencies, dipolar and migration polarization mechanisms dominate, where charges have sufficient time to align or migrate before the field reverses. As the frequency increases, these charged entities (referred to as relaxers) can no longer follow the field rapidly enough, resulting in diminished polarization and hence lower dielectric losses.

Additionally, the low-frequency peaks seen in ε" for Fig. 8(a) and Fig. 8(b) can be associated with interfacial (Maxwell–Wagner–Sillars) polarization, particularly at the interfaces between crystalline and amorphous regions of the HPPE matrix and at the matrix–filler boundaries. These phenomena become more pronounced with increased filler content and play a critical role in determining the dielectric behavior of the composite.

Fig. 9 presents the Cole–Cole plots (imaginary vs. real parts of permittivity) for HPPE/bentonite composites with varying filler content. As observed, the frequency response of these composites deviates from the ideal semicircular arcs predicted by the Debye relaxation model [19], suggesting a non-Debye type relaxation behavior.

In Fig. 9(a) and Fig.9(b), corresponding to composites with 5 wt% and 20 wt% bentonite respectively, the Cole–Cole diagrams display significant distortions at higher frequencies, deviating from the perfect semicircle. These deviations are indicative of a broad distribution of relaxation times, rather than a single, well-defined relaxation time, and may be attributed to heterogeneities in the composite microstructure and interfacial effects. Additionally, contributions from DC conductivity at lower frequencies further skew the diagrams, particularly by elongating the arc horizontally or distorting the low-frequency end [11-15,20].

In contrast, Fig. 8(c), corresponding to the 60 wt% HPPE + 40 wt% bentonite composite, shows characteristics consistent with migration polarization. This behavior is typical in systems with high filler content, where the formation of interfacial regions and space charge accumulation at the matrix–filler interfaces becomes significant. The presence of conductive pathways or percolated filler networks enhances charge transport

across the composite, further deviating from Debye-type relaxation and confirming the role of interfacial and electrode polarization effects in the dielectric response.

The shape and nature of these Cole–Cole plots reinforce the interpretation that, as the bentonite content increases, the dielectric behavior becomes increasingly influenced by interfacial polarization, conductivity effects, and structural heterogeneities, all of which contribute to the complex relaxation dynamics observed in these composites.

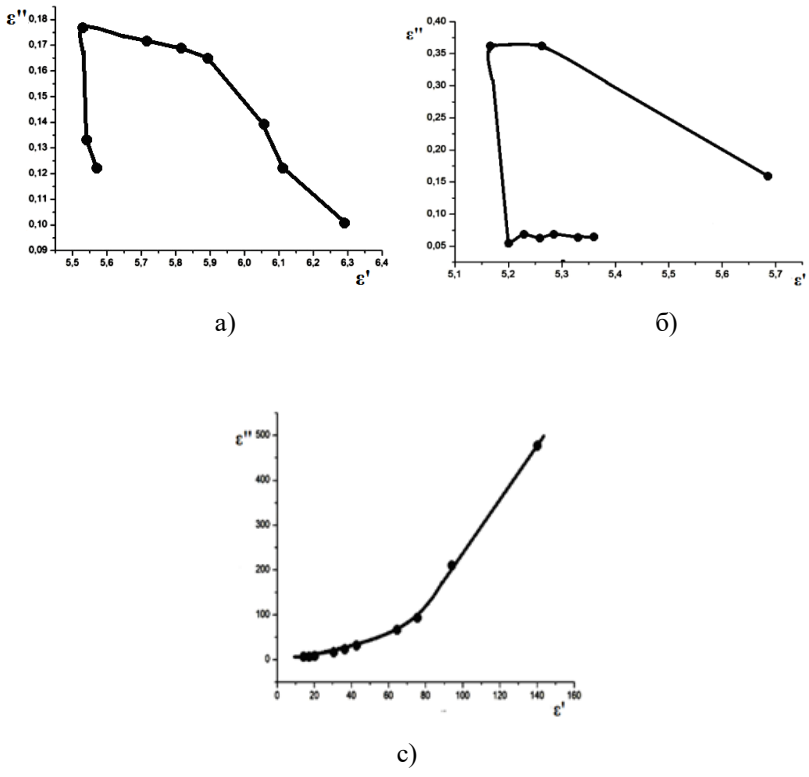

Fig. 9. Cole-Cole diagram for composites: a) 90wt% HPPE + 10wt%B, б) 80 wt% HPPE+ 20 wt%B, c) 30 wt% HPPE +70 wt%B

The temperature dependence of the dielectric properties of the composites is presented in Fig. 9 and Fig. 10, which illustrate the temperature dependence of the permittivity (ε) and the dielectric loss tangent (tgδ) of the studied composites, respectively. Fig. 9 illustrates the variation of permittivity (ε) with temperature, and Fig.10 shows the corresponding behavior of the dielectric loss tangent (tgδ). As observed in Fig. 9, the permittivity exhibits a steady increase with rising temperature, indicating enhanced polarization mechanisms at elevated temperatures. Importantly, the ε(T) dependence does not display any anomalies or abrupt changes that would suggest a relaxation or phase transformation within the temperature range studied.

In contrast, the tgδ(T) behavior is characterized by a more complex, non-monotonic trend. Distinct maxima are observed in the range of 340–350 K, suggesting

the presence of thermally activated processes. These peaks are likely associated with changes in the structural parameters of the interphase boundary layer, which may arise due to phase transitions occurring within the filler crystals. Such transitions can significantly influence charge carrier mobility and interfacial polarization, thereby affecting dielectric loss characteristics at elevated temperatures.

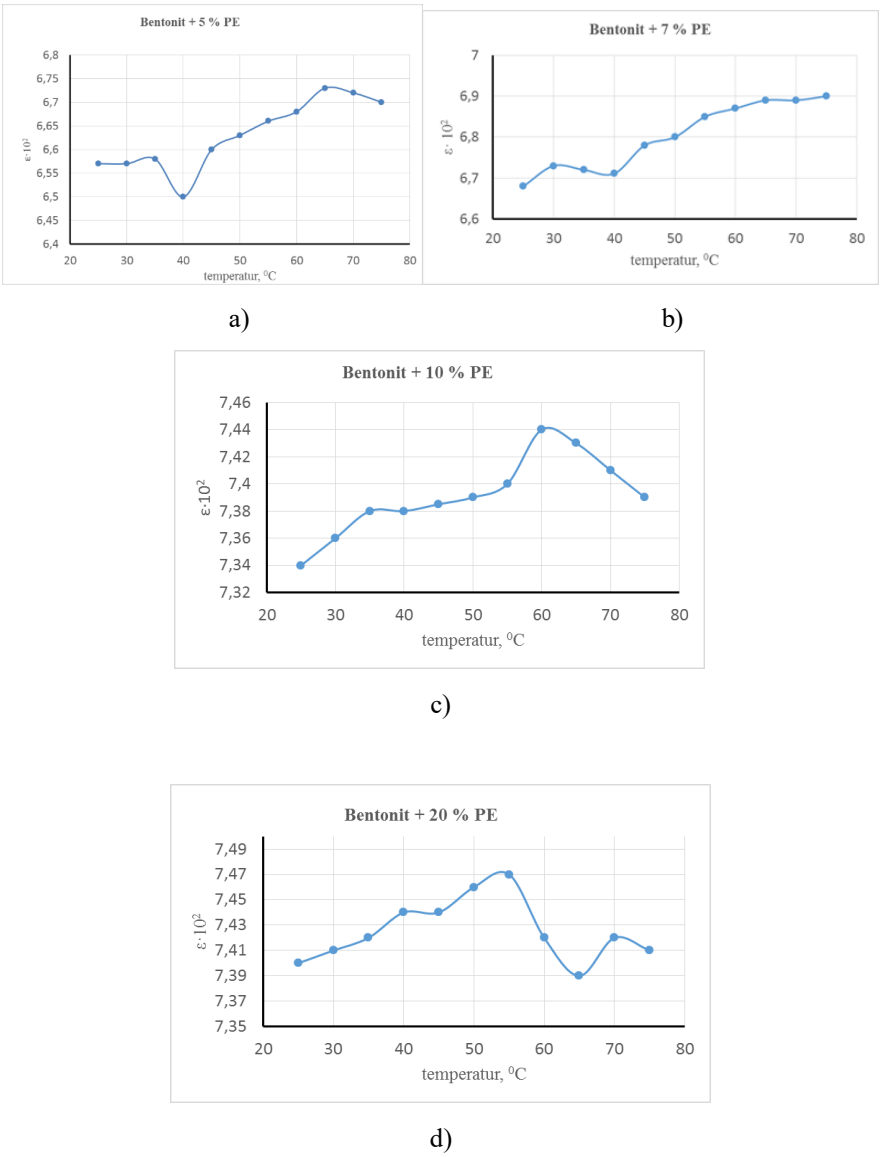

Fig. 10. Temperature dependence of the dielectric permittivity of HPPE + x wt.% (B) composites a) x= 5 wt.%, b) x= 7 wt.%, c) x= 10 wt.% , d) x= 20 wt.%

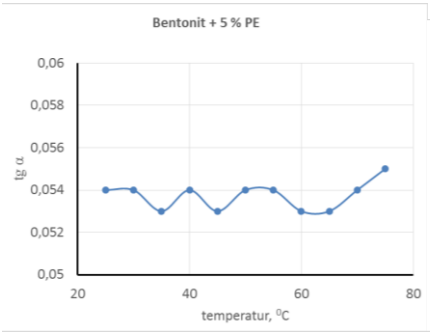

a)

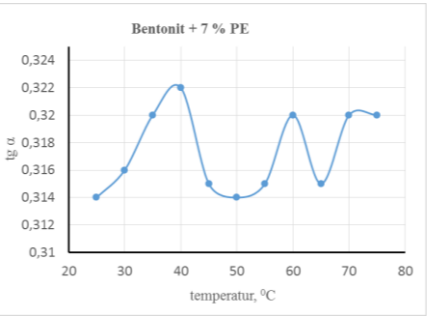

b)

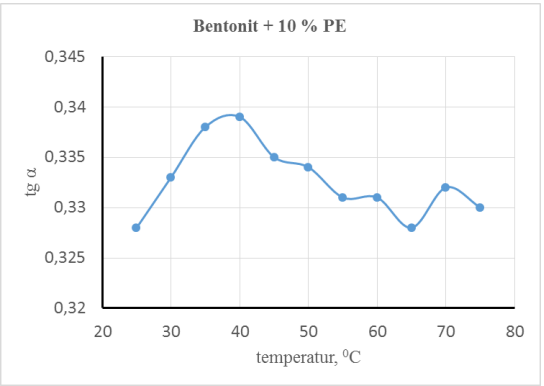

c)

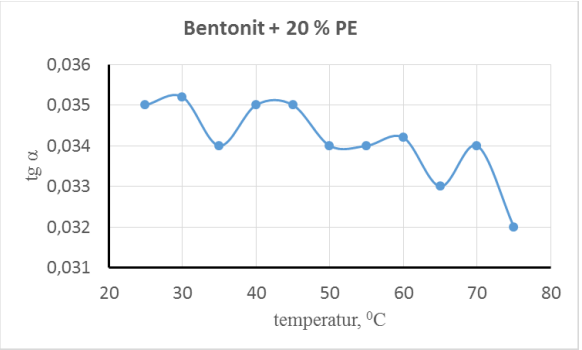

d)

Fig. 11. Temperature dependence of the tangent of the dielectric loss angle of HPPE + x wt.% (B) composites a) x= 5 wt.%, b) x= 7 wt.%, c) x= 10 wt.% , d) x= 20 wt.%

4 Conclusion

In this study, composites based on high-pressure polyethylene (HPPE) reinforced with a bentonite filler were developed and analyzed.

The results showed significant frequency-dependent dispersion of the dielectric parameters. This behavior is attributed to the migration of intrinsic point defects, such as vacancies, interstitial atoms, and structural defects within the filler sublattice. These findings highlight the critical role of both filler content and defect dynamics in determining the electrical performance of HPPE-based composites.

The temperature dependence of the permittivity ε of the composites indicates that permittivity exhibits a steady increase with rising temperature, indicating enhanced polarization mechanisms at elevated temperatures

Dielectric loss tangent behavior is characterized by a more complex, non-monotonic trend. The observed distinct maxima suggested the presence of thermally activated processes and peaks are likely associated with changes in the structural parameters of the interphase boundary layer, which may arise due to phase transitions occurring within the filler crystals.

References

1. Mehrabova M.A., Orujov H.S., Hasanov N.H., Kazimova A.I., Abdullayeva A.A. Ab initio calculations of defects in CdMnSe semimagnetic semiconductors. Mechanics of Solids. **55**, 108–113 (2020)
2. Mehrabova M.A., Madatov R.S.: Calculation of the electron structure of vacancies and their compensated states in III-VI semiconductors. Semiconductors, **45**, 998–1005, (2011)
3. Mehrabova M.A., Nuriyev H.R., Orujov H.S., Nazarov A.M., Sadigov R.M., Poladova V.N. Defect formation energy for charge states and electrophysical properties of CdMnTe. Photonics, Devices, and Systems. **6**, 94500Q (2015)
4. Mehrabova M.A., Sadigov R.M., Nuriyev I.R., Nazarov A.M.: Growth and characterization of epitaxial films based on semimagnetic $Pb_{1-x}Eu_xTe$ solid solutions on various substrates. International Journal of Modern Physics B. **38**(31), 2450419 (2024)
5. Mehrabova M.A., Huseynov N.I., Asadullayeva S.G., Nazarov A.M., Poladova V.N., Suleymanli S.P.: Photoelectrical properties of CdMnSe thin films. **6**(3), 203-210 (2024)
6. Mehrabova M.A., Mammadova S.I., Safarova S.I., Kerimov F.Sh., Mehdiyeva Sh.M. The influence of organic additives phthalic anhydride and phthalic acid on the temperature-time dependencies of the electrical strength of HPPE films. Mechanics of Time-Dependent Materials, (44), 1-9 (2025) https://doi.org/10.1007/s11043-025-09780-1
7. Mehrabova M.A., Mammadova S.I., Kerimov F.Sh., Safarova S.I., Gulmamedov K.J., Hamdillayeva I.H.. Influence of discharges and UV irradiation on the electrical properties of high pressure polyethylene and compositions on its base. Polymer-Plastics Technology and Materials. Taylor and Francis. **63**(16), 2237-2245 (2024) https://doi.org/10.1080/25740881.2024.2369677
8. Mehrabova M.A., Gulmammedov K.J., Safarova S.I. Phase analysis and electrical properties of composites based on high pressure polyethylene with Na+ -montmorillonite filler. Machine science, **2,** 76-82 (2024) https://doi.org/10.61413/GMGO5334
9. Olesik P., Godzierz M., Kozioł M., Jała J., Szeluga U., Myalski J. Structure and mechanical properties of high-density polyethylene composites reinforced with glassy carbon. Materials, **14**(14), 4024 (2021) https://doi.org/10.3390/ma14144024
10. Abduljabbar N., Al-Busaltan Sh., Dulaimi A., Al-Yasari R., Sadique M., Al Nageim H. The effect of waste low-density polyethylene on the mechanical properties of thin asphalt

overlay. Engineering, Materials Science. **315**, 125722 (2021) https://doi.org/10.1016/j.conbuildmat.2021.125722

11. Alim A.A.A., Baharum A., Shirajuddin S.S.M., Anuar F.H.. Blending of low-density polyethylene and poly (Butylene succinate) (LDPE/PBS) with polyethylene–graft–maleic anhydride (PE–g–MA) as a compatibilizer on the phase morphology, mechanical and thermal properties. Polymers (Basel). **15**(2), 261 (2023) https://doi.org/10.3390%2Fpolym15020261
12. Zhi-Jie F., Ping Z., Man-Chao H. Atomic and electronic structures of montmorillonite in soft rock. Chinese Physics B, **18**(7), 2933 (2009) https://doi.org/10.1088/1674-1056/18/7/053
13. Turik A.B., Rodinin M.Yu. Dielectric losses in materials with a limited relaxation time distribution region. JTP Letters. **36**(1), 37–43 (2010) https://cyberleninka.ru/article/n/temperaturno-chastotnaya-dispersiya-dielektricheskih-harakteristik-kompozitov-na-osnove-polietilena-s-vklyucheniyamitlins2/viewer
14. Stadnik A.D., Moroz I.A., Medvedovskaya O.G., Bilyk V.N. Structure and properties of polymer composites and nanocomposites subjected to thermomagnetic treatment. Journal of Nano- and Electronic Physics. **7**(3), 03046-1-03046-5 (2015) http://nbuv.gov.ua/UJRN/jnef_2015_7_3_48
15. Borah D., Nath H., Saikia H. Modification of bentonite clay and its applications. Reviews in Inorganic Chemistry **42**(3), (2021) DOI: 10.1515/revic-2021-0030
16. Lin J., He S., Zhan Y., Zhang Z., Wu X., Yu Y., Zhao, Wang Y. Assessment of sediment capping with zirconium-modified bentonite to intercept phosphorus release from sediments.Environmental Science and Pollution Research **26**(4), 3501–3516 (2019) DOI: 10.1007/s11356-018-3869-y
17. Golebiewski J., Rozanski A., Dzwonkowski J., Galeski A. Low density polyethylene–montmorillonite nanocomposites for film blowing. European Polymer Journal. **44**(2), 270-286 (2008) https://doi.org/10.1016/j.eurpolymj.2007.11.002
18. Thuc Ch., Grillet A., Reinert L., Thuc F., Duclaux L. Separation and purification of montmorillonite and polyethylene oxide modified montmorillonite from Vietnamese bentonites. Applied Clay Science. **49**(3), 229-238 (2010) https://doi.org/10.1016/j.clay.2010.05.011
19. Shugulí M., Rodríguez F., Bruna J., Galotto M., Sarantópoulos C., Perez M., Padula M. Cetylpyridinium bromide-modified montmorillonite as filler in low density polyethylene nanocomposite films. Applied Clay Science. **168,** 203-210 (2019) https://doi.org/10.1016/j.clay.2018.10.020
20. Majeed K., Hassan A., Bakar A., Jawaid M.. Effect of montmorillonite (MMT) content on the mechanical, oxygen barrier, and thermal properties of rice husk/MMT hybrid filler-filled low-density polyethylene nanocomposite blown films. Journal of Thermoplastic Composite Materials.. **29**(7), (2016) https://doi.org/10.1177/0892705714554492
21. Gaska K.. The influence of bentonite content on dielectric and thermal properties of polyethylene-based composites for insulating applications. Materials, **10**(10), 1145 (2017) https://doi.org/10.3390/ma10101145
22. Severino P., Montanheiro T., Ferro O., Passador F., Montanha L. Protective low-density polyethylene residues from prepreg for the development of new nanocomposites with montmorillonite: recycling and characterization. Recycling, **4**(4), 45 (2019) https://doi.org/10.3390/recycling4040045
23. Kumykov E.S., Karmov M.A., Nafonova M.N., Tkhakakhov R.B. et al. Dielectric properties of polymer composites based on SKN-26 and PVC containing nanosized particles. Magazine "Plastic Masses". **3**, 4 (2012). https://www.elibrary.ru/item.asp?id=17743964
24. Mohamed A.T. Experimental enhancement for dielectric strength of polyethylene insulation materials using cost-fewer nanoparticles. International Journal of Electrical Power and Energy Systems. **64**, 469-475 (2015). https://doi.org/10.1016/j.ijepes.2014.06.075
25. Anokwu J. Studies on the effects of bentonite (nanoclay) on the mechanical properties of high-density polyethylene. Journal of Minerals and Materials Characterization and Engineering. **7**(6), 421-434 (2019) doi: 10.4236/jmmce.2019.76029
26. Bartenev G.M., Frenkel S.Y. Physics of polymers. (1990) 432p.

27. Lukichev A.A., Kostyukov N.S. Main features and differences of relaxation and resonance polarization, Bulletin of Amur State University, **25.** 7-11 (2004)
28. Klyndyuk A.I. Surface Phenomenon and Disperse Systems: tutorials for students of chemico-technological specialities. Minsk: BSTU. (2011) 317p.